

NLO QCD corrections to the ($\gamma^* \rightarrow Q\bar{Q}$)-Reggeon vertex

Li-Ping Sun,¹ Long-Bin Chen,² Cong-Feng Qiao,^{3,*} and Kuang-Ta Chao^{4,†}

¹School of Science, Beijing University of Civil Engineering and Architecture, Beijing 100044, China

²School of Physics and Materials Science, Guangzhou University, Guangzhou 510006, China

³College of Physical Sciences, University of Chinese Academy of Sciences, Beijing 100049, China

⁴School of Physics and State Key Laboratory of Nuclear Physics and Technology, Peking University, and Center for High Energy Physics, Peking University, Beijing 100871, China



(Received 25 January 2022; accepted 3 August 2022; published 23 August 2022)

Next-to-leading order (NLO) QCD corrections to the $\gamma^* \rightarrow Q\bar{Q}$ -Reggeon vertex are calculated, where $Q\bar{Q}$ denotes a heavy quark pair $c\bar{c}$ or $b\bar{b}$. The heavy quark mass effects on the photon impact factor are found to be significant, and hence may influence the results of high energy photon-photon scattering and heavy quark pair leptoproduction. In our NLO calculation, similar to the massless case, the ultraviolet (UV) divergences are fully renormalized in the standard procedure, while the infrared (IR) divergences are regulated by the parameter ϵ_{IR} in dimensional regularization. For the process $\gamma^* + q \rightarrow Q\bar{Q} + q$, we calculate all NLO coefficients in terms of ϵ_{IR} , and find they are enhanced due to the heavy quark mass, as compared with the light quark case, and the enhancement factors increase rapidly as the quark mass increases. This might essentially indicate the quark mass effect, in spite of the absence of real corrections that are needed in a complete NLO calculation. Moreover, unlike the γ^* to massless-quark-Reggeon vertex, the results in the present work may apply to the real photon case.

DOI: 10.1103/PhysRevD.106.034027

I. INTRODUCTION

High energy diffractive scattering can be well described by the Pomeron exchange mechanism [1–5]. Within the framework of quantum chromodynamics (QCD), the Balitskii-Fadin-Kuraev-Lipatov (BFKL) Pomeron [6–8], the so-called hard Pomeron, is viewed as the Green's function of two interacting Reggeized gluons with vacuum quantum number, which is evaluated by resuming the leading energy logarithms in perturbative QCD (pQCD) applicable regime, e.g., all $(\alpha_s \ln s)^n$ terms in leading logarithmic approximation (LLA) and all $\alpha_s (\alpha_s \ln s)^n$ terms in the next-to-leading approximation (NLA). People noticed that the virtual photon-photon scattering is an ideal process [9,10] to testify the BFKL predictions and hence the pQCD calculation reliability, which is highly expected in the study of strong interaction physics. The cross section $\sigma_{\text{tot}}^{\gamma^*\gamma^*}$ is calculable in the BFKL approach with relatively high precision and can be realized in experiment through a measurement of the reaction $e^+e^- \rightarrow e^+e^- + X$ by tagging

the outgoing leptons at high energy electron-positron colliders, like LEP and more optimistically CEPC [11] or ILC [12] in the future. Moreover, the recently proposed electron-ion colliders like EIC [13] and EicC [14] may also be good places to study the single diffractive process and hence on small-x physics at lower energies.

Until now, the leading order (LO) BFKL predictions for the $e^+e^- \rightarrow e^+e^- + X$ process have been confronted to the LEP data [15–17], in which the experimental measurement is found above the two-gluon-exchange model result, while below the leading order BFKL Pomeron prediction. Now that the next-to-leading order (NLO) corrections to the BFKL kernel are ready and numerically big and negative [8,18], the higher order corrections may lower the BFKL Pomeron exchange calculation and approach to the experimental measurement. However, in the NLO BFKL calculations, there is still a task remaining: calculating the NLO corrections to the coupling of the BFKL Pomeron and the external photons, which is called photon impact factor [19–21].

The photon impact factor can be obtained by calculating the discontinuity of the process $\gamma^* + \text{Reggeon} \rightarrow \gamma^* + \text{Reggeon}$ process in light of the optical theorem, which tells us that the discontinuity is proportional to the scattering amplitude, $\gamma^* + \text{Reggeon} \rightarrow Q\bar{Q}$, squared. The Reggeon is identified with the elementary t -channel gluons. The NLO corrections to the photon impact factor with massless internal quarks were given in Ref. [22], while here the

* qiaocf@gucas.ac.cn

† ktchao@pku.edu.cn

Published by the American Physical Society under the terms of the Creative Commons Attribution 4.0 International license. Further distribution of this work must maintain attribution to the author(s) and the published article's title, journal citation, and DOI. Funded by SCOAP³.

$Q(\bar{Q})$ are massive quarks, charm, or bottom quarks. In the NLO calculation, analogous to Ref. [22], we calculate the NLO corrections to $\gamma^* + \text{Reggion} \rightarrow Q\bar{Q}$ amplitude on, for example, the left-hand side of the discontinuity line, and the leading $Q\bar{Q}g$ intermediate state on both sides of the discontinuity line. The calculation of the NLO QCD correction hence proceeds in three steps: (i) calculate the NLO corrections to the $\gamma^* + \text{Reggion} \rightarrow Q\bar{Q}$ vertex, (ii) calculate the leading order vertex $\gamma^* + \text{Reggion} \rightarrow Q\bar{Q}g$, and (iii) carry out the integration over the phase space of the intermediate states. In fact, here the calculation procedure is similar to the massless case performed in Ref. [22]. In this paper, as in [22], we give the results of the first step, in which the vertex is extracted from the scattering process $\gamma^* + q \rightarrow Q\bar{Q} + q$ in the high energy limit.

II. TECHNICAL PRELIMINARIES

The kinematics of the $\gamma^* + q \rightarrow Q\bar{Q} + q$ process is illustrated Fig. 1, where q and p are the 4-momenta of photon and incident quark respectively. In the calculation, ϵ represents the polarization vector of the photon, s is the collision energy of the γ^*q system, and m is the mass of the heavy quark. The Lorentz invariants shown include $s = (q+p)^2$, $Q^2 = -q^2$, $t_a = k^2$, $t_b = (q-k-r)^2$, $M^2 = (q+r)^2$, $t = r^2$, and $x = Q^2/2p \cdot q$, the Bjorken scaling variable.

The momenta k and r can be decomposed in the Sudakov form, i.e.,

$$k = \alpha q' + \beta p + k_\perp, \quad (1)$$

$$r = \frac{t}{s} q' - \frac{t_a + t_b - 2m^2}{s} p + r_\perp, \quad (2)$$

with $q' = q + xp$, $q'^2 = p^2 = 0$, and $\beta s = \frac{k^2+m^2}{1-\alpha} - Q^2$.

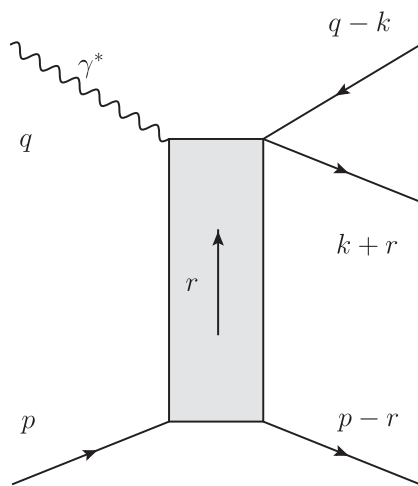


FIG. 1. Kinematics of the process $\gamma^* + q \rightarrow Q\bar{Q} + q$.

The typical Feynman diagrams for NLO corrections are shown in Fig. 2. Of these diagrams, except Fig. 2(n), the upper part quark-antiquark exchange diagrams are implied. For the color octet t -channel configuration, the sum of all diagrams has to be antisymmetric if we interchange the quark and antiquark: $k \rightarrow q - k - r$, $\lambda \rightarrow \lambda'$, where λ, λ' are the helicities of the quark and antiquark, respectively. In particular, the “box” graph shown in Fig. 2(n) has to be antisymmetric by itself. Throughout the calculation, Feynman gauge is employed, and for the t -channel gluons the metric tensor is decomposed into

$$g_{\mu\nu} = \frac{2}{s} (p_\mu q'_\nu + p_\nu q'_\mu) + g_{\mu\nu}^\perp \quad (3)$$

as usual. Note, in practical calculations, the transverse term is not taken into account, whose contributions are suppressed by powers of s . We use the helicity formalism as well, and then our results can be expressed in terms of the following matrix elements similar to [22], i.e.,

$$H_T^a = \bar{u}(k+r, \lambda) \not{p} \not{k} \not{\lambda}^a v(q-k, \lambda'), \quad (4)$$

$$H_\epsilon^a = \bar{u}(k+r, \lambda) \not{\epsilon} \not{\lambda}^a v(q-k, \lambda'), \quad (5)$$

$$H_k^a = \bar{u}(k+r, \lambda) \not{k} \not{\lambda}^a v(q-k, \lambda'), \quad (6)$$

$$H_p^a = \bar{u}(k+r, \lambda) \not{p} \not{\lambda}^a v(q-k, \lambda'), \quad (7)$$

$$H_{ke}^a = \bar{u}(k+r, \lambda) \not{k} \not{\epsilon} \not{\lambda}^a v(q-k, \lambda'), \quad (8)$$

$$H_{pe}^a = \bar{u}(k+r, \lambda) \not{p} \not{\epsilon} \not{\lambda}^a v(q-k, \lambda'), \quad (9)$$

$$H_{pk}^a = \bar{u}(k+r, \lambda) \not{p} \not{k} \not{\lambda}^a v(q-k, \lambda'), \quad (10)$$

$$H_m^a = \bar{u}(k+r, \lambda) \not{\lambda}^a v(q-k, \lambda'). \quad (11)$$

Here λ^a are the generators of the color group. Note that the last four helicity matrix elements do not exist in [22], which always come up with the factor of m .

Taking high energy limit in the calculation, where

$$t, Q^2, t_a, t_b, M^2, m^2 \ll s, \quad (12)$$

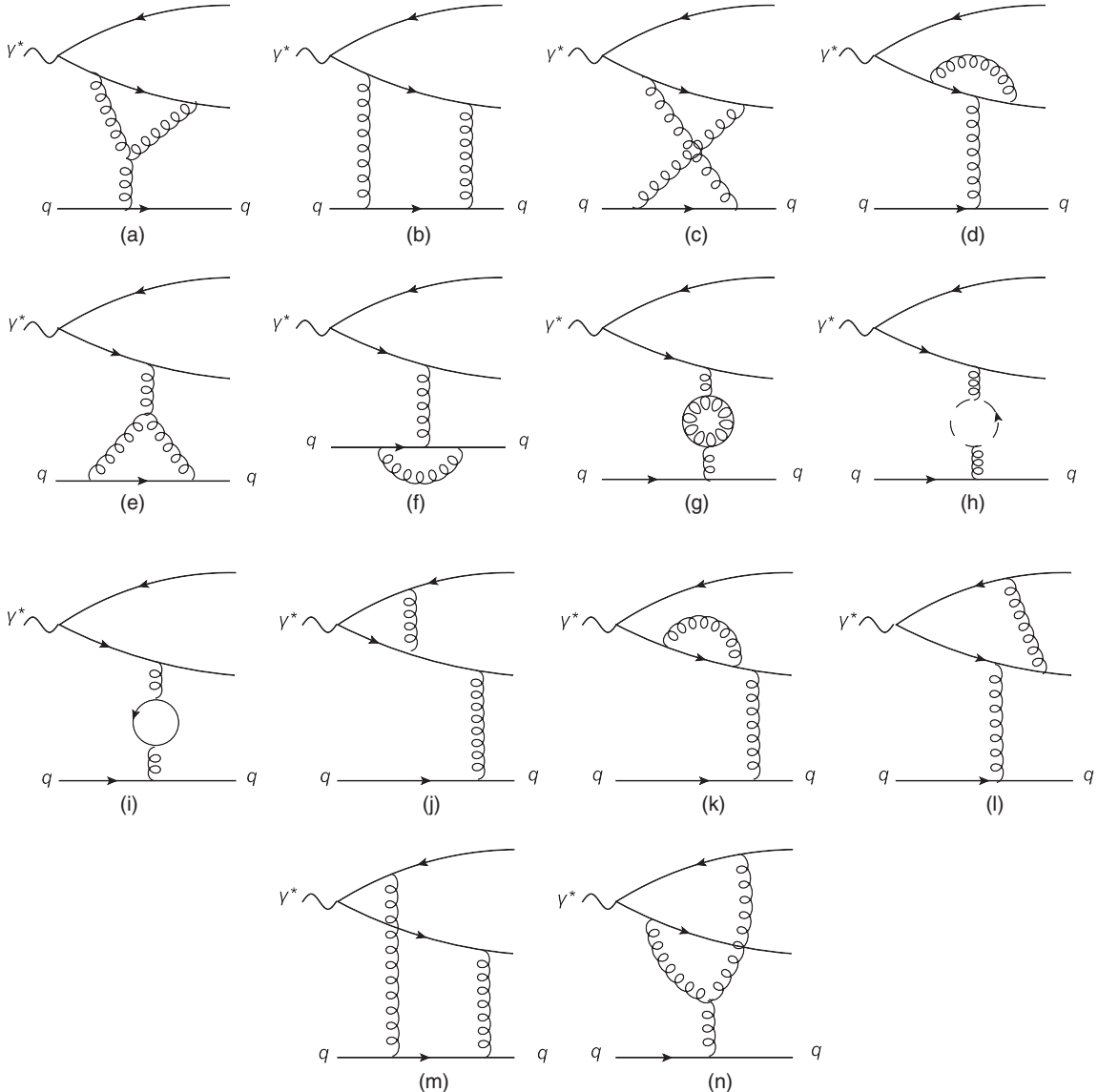
and do not impose any restrictions on the remaining invariants, we then obtain the following amplitude

$$T = g^2 T^{(0)} + g^4 T^{(1)}, \quad (13)$$

with

$$T^{(0)} = \Gamma_{\gamma^* \rightarrow q\bar{q}}^{(0),a} \frac{2s}{t} \Gamma_{qq}^{(0),a}, \quad (14)$$

and

FIG. 2. Feynman diagrams for the process $\gamma^* + q \rightarrow Q\bar{Q} + q$.

$$\Gamma_{qq}^{(0),a} = \frac{1}{s} \bar{u}(p-r, \lambda') q' \lambda^a u(p, \lambda). \quad (15)$$

The only unknown piece of the NLO amplitude is $T^{(1)}$, which corresponds to the processes in Figs. 2(a)–2(n) and will be calculated analytically in the following.

III. CALCULATION METHODS

The method we use in our calculation will be briefly described in the following before presenting the explicit results.

In our calculation the *Mathematica* package FEYNARTS [23] is applied to generate the Feynman diagrams and amplitudes that are relevant to our process. We use FEYNCALC [24] to calculate and simplify the amplitudes. Color in the t -channel is projected onto the antisymmetric

octet as done in [22]. After simplifying the Dirac matrix and employing the Dirac equation of motion, we express the amplitudes as the combination of helicity matrix elements and Passarino-Veltman integrals. For integrals that contain divergences, we separate the divergence part from the finite one. The high energy limit is taken throughout our calculation, i.e., $t, Q^2, t_a, t_b, M^2, m^2 \ll s$.

In this work an extra scale m exists in comparison to [22], and it is too lengthy and redundant to turn all the Passarino-Veltman integrals into scalar integrals or logarithms and dilogarithm functions. For amplitudes that do not contain divergences and high energy scale s , we express them as the combination of Passarino-Veltman integrals and helicity matrix elements. The numerical values of these integrals will be evaluated by LOOPTOOLS [25]. For the pentagon diagram in Fig. 2(n), the reduction method given in [26] is employed to reduce the corresponding integrals to

box integrals. In the end we find our result agrees with that in [22] when taking the $m \rightarrow 0$ limit.

IV. ANALYTIC RESULTS

The NLO amplitudes in $T^{(1)}$ of our concern can be expressed in terms of different diagrams:

$$T^{(1)} = \sum_{i=1}^{13} (A_i + \bar{A}_i) + A_{14}. \quad (16)$$

Here, the subscripts i denote diagrams in Fig. 2, and the amplitudes \bar{A}_i represent those with quark-antiquark interchange in A_i .

A. Results of two- and three-point diagrams

We categorize the diagrams similar to [22]. The results of Fig. 2(a) and its conjugate one are given below, which are split into divergent and finite parts in the $\overline{\text{MS}}$ scheme:

$$\begin{aligned} A_1 = & \frac{N_c}{2} \frac{ee_f}{(4\pi)^{2-\epsilon}} \frac{2}{t(t_a - m^2)} \Gamma_{qq}^{(0),a} \left\{ \frac{3(H_T^a + mH_{pe}^a)c_\Gamma}{\epsilon} + H_T^a[6m^2C_0(1) + 12C_{00}(1)]_{\text{fin}} \right. \\ & + (5m^2 - 2t + 3t_a)C_1(1) + (3m^2 - t + t_a)C_2(1) + 2t_aC_{11}(1) + 2(m^2 - t + t_a)C_{12}(1) \\ & + 2m^2C_{22}(1) - 2] + \alpha s H_e^a[2m^2C_1(1) + (3m^2 - t_a)C_2(1) + 2t_aC_{11}(1) + 2m^2C_{22}(1) \\ & + 2(t_a + m^2)C_{12}(1)] + mH_{pe}^a[3(t_a + m^2)C_0(1) + 12C_{00}(1)]_{\text{fin}} + 2(m^2 - t + 3t_a)C_1(1) \\ & + (3m^2 - 2t + 5t_a)C_2(1) + 2t_aC_{11}(1) + 2(m^2 - t + t_a)C_{12}(1) + 2m^2C_{22}(1) - 2] \\ & \left. + 2\alpha sm H_{ke}^a[C_1(1) + C_2(1) + C_{11}(1) + 2C_{12}(1) + C_{22}(1)] \right\}. \end{aligned} \quad (17)$$

Here $C_i(1) = C_i(t_a, t, m^2, m^2, 0, 0)$ with i the coefficient index. The definitions of all the loop integrals such as C_0 , C_{ij} , D_0 , $D_{i,j,k}$ are standard and given in the Appendix for reference. The subindex fin means the finite part of the loop integrals. Note, the above result does not contain any infrared divergences, while the ultraviolet divergence remains only in $C_{00}(1)$, which can be properly regulated. Numerical evaluation of the finite part may be performed by means of LOOPTOOLS [25] in the $\overline{\text{MS}}$ scheme. The C_i

functions can be reduced into a certain scalar one-loop integral and then expressed as the combination of logarithm and dilogarithm functions. Nevertheless, such kind of reduction may yield a lengthy result and be difficult to read. Due to this reason, we do not perform further reduction on C_i functions; its numerical evaluations are carried by LOOPTOOLS directly.

The result of the conjugate diagram of Fig. 2(a) can be expressed as

$$\begin{aligned} \bar{A}_1 = & \frac{N_c}{2} \frac{ee_f}{(4\pi)^{2-\epsilon}} \frac{2}{t(t_b - m^2)} \Gamma_{qq}^{(0),a} \left\{ \frac{3(H_T^a + mH_{pe}^a - sH_e^a + 2(H_k^a - mH_m^a)\epsilon \cdot p + 2H_p^a\epsilon \cdot r)c_\Gamma}{\epsilon} \right. \\ & + (H_T^a + 2H_p^a\epsilon \cdot r + 2H_k^a\epsilon \cdot p)[6m^2C_0(\bar{1}) + 12C_{00}(\bar{1})]_{\text{fin}} + 2(3m^2 - t + t_b)C_1(\bar{1}) \\ & + (5m^2 - 2t + 3t_b^2)C_2(\bar{1}) + 2m^2C_{11}(\bar{1}) + 2(m^2 - t + t_b)C_{12}(\bar{1}) + 2t_bC_{22}(\bar{1}) - 2] \\ & + sH_e^a[-6m^2C_0(\bar{1}) + (3(\alpha - 3)m^2 + 2t - (1 + \alpha)t_b)C_1(\bar{1}) - 12C_{00}(\bar{1})]_{\text{fin}} \\ & + ((2\alpha - 7)m^2 + 2t - 3t_b)C_2(\bar{1}) + 2(\alpha - 2)m^2C_{11}(\bar{1}) + 2(\alpha - 2)t_bC_{22}(\bar{1}) \\ & + 2((\alpha - 2)m^2 + t + (\alpha - 2)t_b)C_{12}(\bar{1}) + 2] \\ & + 2(\alpha - 1)sm(H_{ke}^a + H_m^a\epsilon \cdot r)[C_1(\bar{1}) + C_2(\bar{1}) + C_{11}(\bar{1}) + 2C_{12}(\bar{1}) + C_{22}(\bar{1})] \\ & + m(H_{pe}^a - 2\epsilon \cdot p H_m^a)[(9m^2 - 3t_b)C_0(\bar{1}) + 12C_{00}(\bar{1})]_{\text{fin}} + (9m^2 - 2t - t_b)C_1(\bar{1}) \\ & \left. + 2(4m^2 - t)C_2(\bar{1}) + 2m^2C_{11}(\bar{1}) + 2(m^2 - t + t_b)C_{12}(\bar{1}) + 2t_bC_{22}(\bar{1}) - 2] \right\}. \end{aligned} \quad (18)$$

Here, $C_i(\bar{1}) = C_i(m^2, t, t_b, m^2, 0, 0)$.

The calculation procedure of Fig. 2(d) is similar to that of Fig. 1, and its result reads:

$$\begin{aligned}
A_4 = & -\frac{1}{2N_c} \frac{ee_f}{(4\pi)^{2-\epsilon}} \frac{4}{t(t_a - m^2)} \Gamma_{qq}^{(0),a} \left\{ \frac{(H_T^a + mH_{pe}^a)c_\Gamma}{2\epsilon} + H_T^a[(m^2 - t + t_a)C_0(4) \right. \\
& + (3m^2 - t + t_a)C_1(4) + (2m^2 - t + 2t_a)C_2(4) + 2C_{00}(4)_{\text{fin}} + m^2C_{11}(4) \\
& + (m^2 - t + t_a)C_{12}(4) + t_aC_{22}(4) - 1] + \alpha s H_\epsilon^a [(m^2 - t_a)C_0(4) - t_aC_1(4) \\
& + (m^2 - 2t_a)2C_2(4) - m^2C_{11}(4) - (t_a + m^2)C_{12}(4) - t_aC_{22}(4)] \\
& + mH_{pe}^a [(2t_a - t)C_0(4) + (2m^2 - t + 2t_a)C_1(4) + (m^2 - t + 3t_a)C_2(4) \\
& + 2C_{00}(4)_{\text{fin}} + m^2C_{11}(4) + (m^2 - t + t_a)C_{12}(4) + t_aC_{22}(4) - 1] \\
& \left. - \alpha s m H_{ke}^a [C_1(4) + C_2(4) + C_{11}(4) + 2C_{12}(4) + C_{22}(4)] \right\}, \tag{19}
\end{aligned}$$

where $C_i(4) = C_i(m^2, t, t_a, 0, m^2, m^2)$.

The result of the conjugate diagram of Fig. 2(d) is

$$\begin{aligned}
\bar{A}_4 = & -\frac{1}{2N_c} \frac{ee_f}{(4\pi)^{2-\epsilon}} \frac{4}{t(t_b - m^2)} \Gamma_{qq}^{(0),a} \left\{ \frac{(H_T^a + mH_{pe}^a - sH_\epsilon^a + 2(H_k^a - mH_m^a)\epsilon \cdot p + 2H_p^a\epsilon \cdot r)c_\Gamma}{2\epsilon} \right. \\
& + H_T^a[(m^2 - t + t_b)C_0(\bar{4}) + (3m^2 - t + t_b)C_1(\bar{4}) + (2m^2 - t + 2t_b)C_2(\bar{4}) \\
& + 2C_{00}(\bar{4})_{\text{fin}} + m^2C_{11}(\bar{4}) + (m^2 - t + t_b)C_{12}(\bar{4}) + t_bC_{22}(\bar{4}) - 1] \\
& + sH_\epsilon^a [((\alpha - 2)m^2 + t - \alpha t_b)C_0(\bar{4}) + (t - 3m^2 - \alpha t_b)C_1(\bar{4}) \\
& + ((\alpha - 3)m^2 + t - 2\alpha t_b)C_2(\bar{4}) - 2C_{00}(\bar{4})_{\text{fin}} - \alpha m^2C_{11}(\bar{4}) \\
& + (t - \alpha m^2 - \alpha t_b)C_{12}(\bar{4}) - \alpha t_bC_{22}(\bar{4}) + 1] \\
& + 2(H_k^a\epsilon \cdot p + H_p^a\epsilon \cdot r)[(m^2 - t + t_b)C_0(\bar{4}) + 2C_{00}(\bar{4})_{\text{fin}} \\
& + (3m^2 - t + t_b)C_1(\bar{4}) + (2m^2 - t + 2t_b)C_2(\bar{4}) + m^2C_{11}(\bar{4}) \\
& + (m^2 - t + t_b)C_{12}(\bar{4}) + t_bC_{22}(\bar{4}) - 1] \\
& + m(H_{pe}^a + 2H_m^a\epsilon \cdot p)[(2m^2 - t)C_0(\bar{4}) + (4m^2 - t)C_1(\bar{4}) + (3m^2 - t + t_b)C_2(\bar{4}) \\
& + 2C_{00}(\bar{4})_{\text{fin}} + m^2C_{11}(\bar{4}) + (m^2 - t + t_b)C_{12}(\bar{4}) + t_bC_{22}(\bar{4}) - 1] \\
& \left. + (1 - \alpha)m(H_{ke}^a + 2H_m^a\epsilon \cdot r)[C_1(\bar{4}) + C_2(\bar{4}) + C_{11}(\bar{4}) + 2C_{12}(\bar{4}) + C_{22}(\bar{4})] \right\}, \tag{20}
\end{aligned}$$

with $C_i(\bar{4}) = C_i(m^2, t, t_b, 0, m^2, m^2)$.

The diagrams in Figs. 2(e) and 2(f) belong to the NLO corrections to the lower vertex $\Gamma_{qq}^{(1),a}$. Their results are

$$A_5 = -N_c \frac{ee_f}{(4\pi)^{2-\epsilon}} \frac{2}{t(t_a - m^2)} \Gamma_{qq}^{(0),a} (H_T^a + mH_{pe}^a) c_\Gamma \left\{ \frac{(-t)^{-\epsilon}}{2\epsilon} + 1 \right\}, \tag{21}$$

and

$$A_6 = \frac{1}{2N_c} \frac{ee_f}{(4\pi)^{2-\epsilon}} \frac{2}{t(t_a - m^2)} \Gamma_{qq}^{(0),a} (H_T^a + mH_{pe}^a) c_\Gamma (-t)^{-\epsilon} \left\{ \frac{2}{\epsilon^2} + \frac{3}{\epsilon} + 8 \right\}. \tag{22}$$

In the zero mass limit, it is obvious that these two amplitudes are just Eqs. (35) and (36) in [22].

Figures 2(g)–2(i) contribute to both the upper and lower vertices, and we find

$$A_{7+8} = \frac{ee_f}{(4\pi)^{2-\epsilon}} \frac{2N_c c_\Gamma (-t)^{-\epsilon}}{t(t_a - m^2)} \Gamma_{qq}^{(0),a} (H_T^a + mH_{pe}^a) \left(\frac{5}{3\epsilon} + \frac{31}{9} \right), \tag{23}$$

and

$$A_9 = -n_f \frac{ee_f}{(4\pi)^{2-\epsilon}} \frac{2c_\Gamma(-t)^{-\epsilon}}{t(t_a - m^2)} \Gamma_{qq}^{(0),a} (H_T^a + mH_{pe}^a) \left(\frac{2}{3\epsilon} + \frac{10}{9} \right). \quad (24)$$

The results of conjugate diagrams of Figs. 2(e)–2(i) can readily be obtained by substituting $(H_T^a + mH_{pe}^a)$ with $(H_T^a + mH_{pe}^a - sH_e^a + 2(H_k^a - mH_m^a)\epsilon \cdot p + 2H_p^a\epsilon \cdot r)$ and making the replacement $t_a \rightarrow t_b$.

The result of vertex correction diagram Fig. 2(j) can be expressed as follows:

$$\begin{aligned} A_{10} = & -\frac{C_F ee_f}{(4\pi)^{2-\epsilon}} \frac{4}{t(t_a - m^2)} \Gamma_{qq}^{(0),a} \left\{ \frac{-(H_T^a + mH_{pe}^a)c_\Gamma}{2\epsilon} + H_T^a[m^2C_0(10) + Q^2C_2(10)] \right. \\ & + (m^2 + Q^2 + t_a)C_1(10) - 2C_{00}(10)_{\text{fin}} - m^2C_{11}(10) + (Q^2 + t_a - m^2)C_{12}(10) \\ & + Q^2C_{22}(10) + 1] + mH_{pe}^a[m^2C_0(10) + (Q^2 + 2t_a)C_1(10) + Q^2C_2(10) \\ & - 2C_{00}(10)_{\text{fin}} - m^2C_{11}(10) + (Q^2 - m^2 + t_a)C_{12}(10) + Q^2C_{22}(10) + 1] \\ & + 2\epsilon \cdot k[(m(2mH_p^a + H_{pk}^a) - t_a H_p^a)C_1(10) + m(mH_p^a + H_{pk}^a)C_{11}(10) \\ & \left. + H_p^a(m^2 - t_a)C_{12}(10)] \right\}. \end{aligned} \quad (25)$$

Here $C_i(10) = C_i(m^2, t_a, -Q^2, m^2, 0, m^2)$.

The NLO amplitude of the conjugate diagram of Fig. 2(j) is

$$\begin{aligned} \bar{A}_{10} = & -\frac{C_F ee_f}{(4\pi)^{2-\epsilon}} \frac{4}{t(t_b - m^2)} \Gamma_{qq}^{(0),a} \left\{ \frac{(H_T^a + mH_{pe}^a - sH_e^a + 2(H_k^a - mH_m^a)\epsilon \cdot p + 2H_p^a\epsilon \cdot r)c_\Gamma}{2\epsilon} \right. \\ & + (H_T^a - sH_e^a + 2H_k^a\epsilon \cdot p)[m^2C_0(\overline{10}) + (m^2 + Q^2 + t_b)C_1(\overline{10}) + Q^2C_2(\overline{10})] \\ & - 2C_{00}(\overline{10})_{\text{fin}} - m^2C_{11}(\overline{10}) + (Q^2 - m^2 + t_b)C_{12}(\overline{10}) + Q^2C_{22}(\overline{10}) + 1] \\ & + mH_{pe}^a[m^2C_0(\overline{10}) + (2m^2 + Q^2)C_1(\overline{10}) + Q^2C_2(\overline{10}) - 2C_{00}(\overline{10})_{\text{fin}} - m^2C_{11}(\overline{10}) \\ & + (Q^2 - m^2 + t_b)C_{12}(\overline{10}) + Q^2C_{22}(\overline{10}) + 1] + 2H_{pk}^a[C_1(\overline{10}) + C_{11}(\overline{10})] \\ & \times (\epsilon \cdot r + \epsilon \cdot k) + 2mH_p^a[((2m^2 - t_b)C_1(\overline{10}) + m^2C_{11}(\overline{10}) + (m^2 - t_b)C_{12}(\overline{10}))\epsilon \cdot k \\ & + (m^2C_0(\overline{10}) + (3m^2 + Q^2)C_1(\overline{10}) + Q^2C_2(\overline{10}) - 2C_{00}(\overline{10})_{\text{fin}} + Q^2C_{12}(\overline{10}) \\ & + Q^2C_{22}(\overline{10}) + 1)\epsilon \cdot r] + 2mH_m^a[(-m^2C_0(\overline{10}) - (2m^2 + Q^2)C_1(\overline{10}) - Q^2C_2(\overline{10}) \\ & + 2C_{00}(\overline{10})_{\text{fin}} + m^2C_{11}(\overline{10}) + (m^2 - Q^2 - t_b)C_{12}(\overline{10}) - Q^2C_{22}(\overline{10}) - 1)\epsilon \cdot p \\ & \left. - s(C_1(\overline{10}) + C_{11}(\overline{10}))(\epsilon \cdot r + \epsilon \cdot k)] \right\}, \end{aligned} \quad (26)$$

with $C_i(\overline{10}) = C_i(m^2, t_b, -Q^2, m^2, 0, m^2)$.

The result of the quark self-energy diagram Fig. 2(k) is

$$\begin{aligned} A_{11} = & \frac{ee_f}{(4\pi)^{2-\epsilon}} \frac{2C_F c_\Gamma}{t(t_a - m^2)^2} \Gamma_{qq}^{(0),a} \left\{ \frac{(7m^2 - t_a)H_T^a + 2(t_a + 2m^2)mH_{pe}^a}{\epsilon} \right. \\ & + \ln(m^2)[(t_a - 7m^2)H_T^a - 2(t_a + 2m^2)mH_{pe}^a] + \frac{4t_a(t_a + m^2)mH_{pe}^a - (m^4 - 10t_a m^2 + t_a^2)H_T^a}{t_a} \\ & \left. + \frac{\ln(1 - \frac{t_a}{m^2})(t_a - m^2)((m^4 - 6t_a m^2 + t_a^2)H_T^a - 2t_a(t_a + m^2)mH_{pe}^a)}{t_a^2} \right\} \end{aligned} \quad (27)$$

and the amplitude of the conjugate diagram of Fig. 2(k) reads

$$\bar{A}_{11} = \frac{ee_f}{(4\pi)^{2-\epsilon}} \frac{2C_F c_\Gamma}{t(t_b - m^2)^2} \Gamma_{qq}^{(0),a} \left\{ \frac{(7m^2 - t_b)(H_T^a - sH_\epsilon^a + 2H_k^a \epsilon \cdot p + 2H_p^a \epsilon \cdot r)}{\epsilon} + \frac{2(5m^2 - 2t_b)m(H_{pe}^a - 2H_m^a \epsilon \cdot p)}{\epsilon} \right. \\ \left. + \frac{1}{t_a} \left[(H_T^a - sH_\epsilon^a + 2H_k^a \epsilon \cdot p + 2H_p^a \epsilon \cdot r) \left(-t_b(7m^2 - t_b) \ln(m^2) - \frac{m^2 - t_b}{t_b} (m^4 - 6m^2 t_b + t_b^2) \ln\left(\frac{m^2 - t_b}{m^2}\right) \right. \right. \right. \\ \left. \left. \left. - m^4 + 10m^2 t_b - t_b^2 \right) + 2m(H_{pe}^a - 2H_m^a \epsilon \cdot p) \left(-t_b(5m^2 - 2t_b) \ln(m^2) \right. \right. \right. \\ \left. \left. \left. - \frac{m^2 - t_b}{t_b} (m^4 - 5m^2 t_b + 2t_b^2) \ln\left(\frac{m^2 - t_b}{m^2}\right) - m^4 + 8m^2 t_b - 3t_b^2 \right) \right] \right\}. \quad (28)$$

B. The box diagrams

Here, we present the results of box diagrams. In the calculation of diagrams in Figs. 2(b) and 2(c), the four-point integrals have to be considered. After taking the high energy limit and eliminating the s suppressed terms, in the end the results turn out to be quite simple, that is

$$A_{2+3} = \frac{ee_f N_c}{(4\pi)^{2-\epsilon}} \frac{c_\Gamma}{t(t_a - m^2)} \Gamma_{qq}^{(0),a} (H_T^a + mH_{pe}^a) \left\{ \frac{(-t)^{-\epsilon}}{\epsilon^2} - \frac{3(m^2)^{-\epsilon}}{2\epsilon^2} + \frac{(m^2)^{-\epsilon}}{\epsilon} \left(\ln\left(-\frac{\alpha s}{m^2}\right) + \ln\left(\frac{\alpha s}{m^2}\right) + \ln\left(\frac{-t}{m^2}\right) \right. \right. \\ \left. \left. - \ln\left(1 - \frac{t_a}{m^2}\right) \right) - \ln\left(-\frac{t}{m^2}\right) \left[\ln\left(-\frac{\alpha s}{m^2}\right) + \ln\left(\frac{\alpha s}{m^2}\right) \right] - \ln\left(1 - \frac{t_a}{m^2}\right)^2 - \frac{3\pi^2}{4} + C_0(1) \right\}. \quad (29)$$

Here, $C_0(1) = C_0(t_a, t, m^2, m^2, 0, 0)$, as in A_1 .

The results of diagrams conjugating to Figs. 2(b) and 2(c) can be obtained by taking the following replacements: $t_a \rightarrow t_b$, $\alpha \rightarrow 1 - \alpha$, $(H_T^a + mH_{pe}^a) \rightarrow (H_T^a + mH_{pe}^a - sH_\epsilon^a + 2(H_k^a - mH_m^a)\epsilon \cdot p + 2H_p^a \epsilon \cdot r)$.

Note that there are $\ln s$ terms in the amplitudes of Figs. 2(b) and 2(c), and also their conjugate partners.

Next, we give the result of the adjacent box as shown in Fig. 2(l),

$$A_{12} = \Gamma_{qq}^{(0),a} \frac{2s}{t} \left(\frac{ee_f}{s} \right) \left(-\frac{1}{2N_c} \right) \frac{2}{(4\pi)^{2-\epsilon}} \left\{ \frac{c_\Gamma}{\epsilon} A_{12}^{-1} + A_{12}^0 \right\}, \quad (30)$$

in which the divergent part A_{12}^{-1} is

$$A_{12}^{-1} = -(H_T^a + mH_{pe}^a) \frac{M^2 x_r \ln(x_r)}{m^2(1 - x_r^2)}, \quad (31)$$

with

$$x_r = -\frac{1 - \sqrt{1 - \frac{4m^2}{2m^2 + M^2}}}{1 + \sqrt{1 - \frac{4m^2}{2m^2 + M^2}}}, \quad (32)$$

and $M^2 = (q + r)^2$, defined in the above paragraph.

The finite term A_{12}^0 is given in the Appendix. The amplitude of the conjugate diagram of Fig. 2(l) goes as

$$\bar{A}_{12} = \Gamma_{qq}^{(0),a} \frac{2s}{t} \left(\frac{ee_f}{s} \right) \left(-\frac{1}{2N_c} \right) \frac{2}{(4\pi)^{2-\epsilon}} \left\{ \frac{c_\Gamma}{\epsilon} \bar{A}_{12}^{-1} + \bar{A}_{12}^0 \right\}, \quad (33)$$

where the divergent term

$$\bar{A}_{12}^{-1} = -\frac{M^2 x_r \ln(x_r)}{m^2(1 - x_r^2)} [H_T^a + mH_{pe}^a - sH_\epsilon^a + 2(H_k^a - mH_m^a)\epsilon \cdot p + 2H_p^a \epsilon \cdot r]. \quad (34)$$

The finite piece is also given in the Appendix.

The opposite box diagram Fig. 2(n) does not contain any divergence, its lengthy analytic expression is presented in the Appendix.

C. The pentagon diagram

In this subsection we deal with the pentagon diagram Fig. 2(m). The calculation procedure is complicated and is performed by computer algebra. Due to the fact that the integrals depend upon the large scale s , they can be greatly simplified in the high energy limit. The results are as follows:

$$A_{13} = \Gamma_{qq}^{(0),a} \frac{N_c}{2} \frac{ee_f}{t(4\pi)^{2-\epsilon}} \left\{ \frac{1}{\epsilon^2} A_{13}^{(-2)} + \frac{1}{\epsilon} A_{13}^{(-1)} + \frac{A_{13}^{(0)}}{\Delta} \right\}. \quad (35)$$

Here,

$$\Delta = \alpha(\alpha - 1)m^4 - m^2(t + \alpha(\alpha - 1)(t_a + t_b)) + \alpha(\alpha - 1)(Q^2t + t_a t_b), \quad (36)$$

$$A_{13}^{(-2)} = \left\{ -(H_T^a + mH_{pe}^a) \left[\frac{1}{t_a - m^2} + \frac{1}{t_b - m^2} \right] + \frac{sH_e^a - 2(H_k^a - mH_m^a)\epsilon \cdot p - 2H_p^a\epsilon \cdot r}{t_b - m^2} \right\}, \quad (37)$$

and

$$A_{13}^{(-1)} = 2 \left\{ (H_T^a + mH_{pe}^a) \left[\ln(m) \left(\frac{1}{t_a - m^2} + \frac{1}{t_b - m^2} \right) + \frac{\ln(1 - \frac{t_a}{m^2})}{t_a - m^2} + \frac{\ln(1 - \frac{t_b}{m^2})}{t_b - m^2} \right. \right. \\ \left. \left. + \frac{(t_b - t_a) \ln(\frac{\alpha-1}{\alpha})}{(t_a - m^2)(t_b - m^2)} \right] - \frac{sH_e^a - 2(H_k^a - mH_m^a)\epsilon \cdot p - 2H_p^a\epsilon \cdot r}{t_b - m^2} \ln \left(\frac{(t_a - m^2)\alpha}{m(1 - \alpha)} \right) \right\}. \quad (38)$$

The finite piece $A_{13}^{(0)}$ in (35) is listed in the Appendix. Note, we can reproduce the massless result [22] when taking the $m \rightarrow 0$ limit in the above expressions.

We can obtain the amplitude of the conjugate diagram of Fig. 2(m) by replacing $s \rightarrow -s$ in the $D_0(1)$, $D_0(2)$, $D_0(3)$, $D_0(4)$, and $D_i(14) \rightarrow -D_i(14)$. With these replacements one can easily find that the energy dependence $\ln s$ terms in Fig. 2(m) cancel the terms in its conjugate diagram. Therefore, the energy dependence terms merely come from $A_{2+3} + \bar{A}_{2+3}$.

For convenience, we give all the results derived from *Mathematica*, which are in [27].

V. RENORMALIZATION

The results of our considered process contain both infrared and ultraviolet divergences. The ultraviolet divergences may be renormalized via standard procedure, i.e., canceled by counterterms, in modified minimal subtraction ($\overline{\text{MS}}$) scheme here. The infrared divergences may be canceled out when the soft gluon radiation process $\gamma^* + \text{Reggeon} \rightarrow Q\bar{Q}g$ is taken into account.

The ultraviolet divergences exist only in the self-energy and triangle diagrams, which are

$$A_1^{\text{UV}} = \frac{ee_f}{(4\pi)^{2-\epsilon}} \frac{2(H_T^a + mH_{pe}^a)}{t(t_a - m^2)} \Gamma_{qq}^{(0),a} \frac{3N_c c_\Gamma}{2\epsilon_{\text{UV}}}, \quad (39)$$

$$A_4^{\text{UV}} = \frac{ee_f}{(4\pi)^{2-\epsilon}} \frac{2(H_T^a + mH_{pe}^a)}{t(t_a - m^2)} \Gamma_{qq}^{(0),a} \left(-\frac{c_\Gamma}{2N_c \epsilon_{\text{UV}}} \right), \quad (40)$$

$$A_5^{\text{UV}} = \frac{ee_f}{(4\pi)^{2-\epsilon}} \frac{2(H_T^a + mH_{pe}^a)}{t(t_a - m^2)} \Gamma_{qq}^{(0),a} \frac{3N_c c_\Gamma}{2\epsilon_{\text{UV}}}, \quad (41)$$

$$A_6^{\text{UV}} = \frac{ee_f}{(4\pi)^{2-\epsilon}} \frac{2(H_T^a + mH_{pe}^a)}{t(t_a - m^2)} \Gamma_{qq}^{(0),a} \left(-\frac{c_\Gamma}{2N_c \epsilon_{\text{UV}}} \right), \quad (42)$$

$$A_{7+8+9}^{\text{UV}} = \frac{ee_f}{(4\pi)^{2-\epsilon}} \frac{2(H_T^a + mH_{pe}^a)}{t(t_a - m^2)} \Gamma_{qq}^{(0),a} \frac{c_\Gamma}{\epsilon_{\text{UV}}} \left(\frac{5}{3}N_c - \frac{2}{3}n_f \right), \quad (43)$$

$$A_{10}^{\text{UV}} = \frac{ee_f}{(4\pi)^{2-\epsilon}} \frac{2(H_T^a + mH_{pe}^a)}{t(t_a - m^2)} \Gamma_{qq}^{(0),a} \frac{c_\Gamma}{\epsilon_{\text{UV}}} C_F, \quad (44)$$

and

$$A_{11}^{\text{UV}} = \frac{ee_f}{(4\pi)^{2-\epsilon}} \frac{2}{t(t_a - m^2)^2} \Gamma_{qq}^{(0),a} \frac{c_\Gamma}{\epsilon_{\text{UV}}} 2C_F((7m^2 - t_a)H_T^a \\ + 2(t_a + 2m^2)mH_{pe}^a). \quad (45)$$

For the ultraviolet divergence discussed above, when taking the massless limit we can find it is in agreement with the result in [22]. We denote Z_2 , Z_3 , Z_m , Z_g as the quark-field, gluon-field, mass, and coupling renormalization constants, respectively. Note, in our calculation the renormalization constants Z_2 and Z_m are defined in an on-shell scheme, while Z_3 and Z_g are given in a $\overline{\text{MS}}$ scheme, which tells us

$$Z_2 = 1 - \frac{\alpha_s}{4\pi} C_F \left[\frac{1}{\epsilon_{\text{UV}}} + \frac{2}{\epsilon_{\text{UV}}} - 3\gamma_E + 3 \ln \left(\frac{4\pi\mu^2}{m^2} \right) + 4 \right], \quad (46)$$

$$Z_3 = 1 + \frac{\alpha_s}{4\pi} \left(\frac{5}{3}N_c - \frac{2}{3}n_f \right) \left[\frac{1}{\epsilon_{\text{UV}}} - \gamma_E + \ln(4\pi) \right], \quad (47)$$

$$Z_g = 1 - \frac{\alpha_s}{4\pi} \left(\frac{11}{6}N_c - \frac{1}{3}n_f \right) \left[\frac{1}{\epsilon_{\text{UV}}} - \gamma_E + \ln(4\pi) \right], \quad (48)$$

and

$$Z_m = 1 - 3 \frac{\alpha_s}{4\pi} C_F \left[\frac{1}{\epsilon_{\text{UV}}} - \gamma_E + \ln \left(\frac{4\pi\mu^2}{m^2} \right) + \frac{4}{3} \right]. \quad (49)$$

After including the counterterms, all of the above ultraviolet divergences and those divergences from their conjugate diagrams are canceled out. Hence our results will be ultraviolet finite.

VI. NUMERICAL RESULTS

In the following we show the mass effect numerically in NLO corrections of the photon impact factor. Since in this work the infrared divergences still exist, the NLO amplitude squared can be expressed as

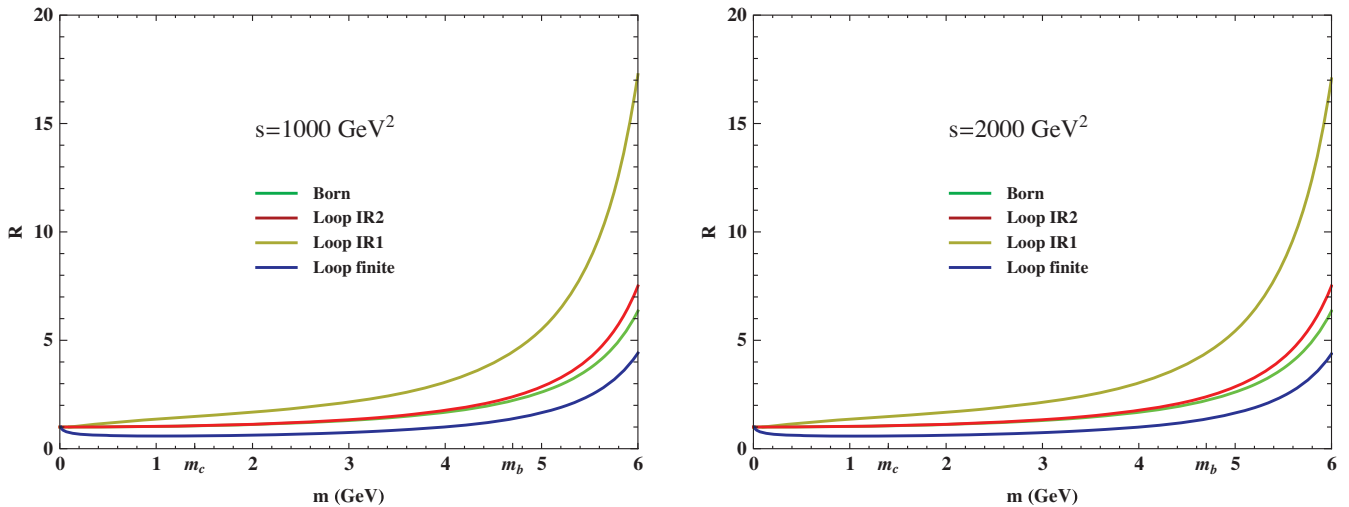


FIG. 3. The ratios of $|M|_{\text{Born}}^2$, $|M|_{\text{Loop IR2}}^2$, $|M|_{\text{Loop IR1}}^2$, and $|M|_{\text{Loop finite}}^2$ versus the quark mass in the process $\gamma^* + q \rightarrow Q\bar{Q} + q$.

$$\begin{aligned} |M_{\text{NLO}}|^2 &= M_{\text{NLO}} M_{\text{LO}}^* = (M_{\text{Born}} + M_{\text{Loop}}) M_{\text{LO}}^* \\ &= |M_{\text{Born}}|^2 + \frac{1}{\epsilon^2} |M_{\text{Loop IR2}}|^2 + \frac{1}{\epsilon} |M_{\text{Loop IR1}}|^2 \\ &\quad + |M_{\text{Loop finite}}|^2. \end{aligned} \quad (50)$$

We then can evaluate respectively the mass effects for the Born term $|M|_{\text{Born}}^2$, second-order infrared divergent term $|M|_{\text{Loop IR2}}^2$, first-order infrared divergent term $|M|_{\text{Loop IR1}}^2$, and NLO finite term $|M|_{\text{Loop finite}}^2$.

In the numerical evaluation, we take the following inputs:

$$\begin{aligned} n_f &= 5, & Q &= 7 \text{ GeV}, & \mu &= Q^2, \\ \alpha &= 0.2, & t_a &= t_b &= t &= 50 \text{ GeV}^2. \end{aligned} \quad (51)$$

In our calculation, the quark mass m varies from 0 to 6 GeV, then $n_f = 5$ (in the physical world the charm quark mass and bottom quark mass are about 1.4 and 4.7 GeV, respectively). In order to demonstrate the results more clearly, we define the ratio $R(m) = \frac{|M|^2}{|M|_{m=0 \text{ GeV}}^2}$, and the ratios of $|M|_{\text{Born}}^2$, $|M|_{\text{Loop UV}}^2$, $|M|_{\text{Loop IR2}}^2$, $|M|_{\text{Loop IR1}}^2$, and $|M|_{\text{Loop finite}}^2$. The inputs s are taken as $s = 1000 \text{ GeV}^2$ and $s = 2000 \text{ GeV}^2$, respectively. The curves are shown in Fig. 3.

From Fig. 3 we can see that, for $s = 1000 \text{ GeV}^2$ and $s = 2000 \text{ GeV}^2$, the curves change little. As the quark mass gets larger, the NLO amplitude squared also gets larger quickly, even for the $|M|_{\text{Loop IR1}}^2$, the ratio is nearly 20 when the quark mass is 6 GeV. So we may conclude that, in the $\gamma^* \rightarrow Q\bar{Q}$ -Reggeon vertex, the quark mass effects on the photon impact factor are significant, and may influence the results of high energy photon-photon scattering and heavy quark pair leptoproduction.

VII. CONCLUSIONS

In this paper, we calculated the process $\gamma^* + q \rightarrow Q\bar{Q} + q$ at NLO with fully virtual corrections in the high energy limit for massive quark pair $Q(\bar{Q})$, which tells the coupling of the Reggeized gluon to $\gamma^* \rightarrow Q\bar{Q}$. This calculation is just the first step of our final purpose, to obtain the complete NLO corrections to the photon impact factor and checking the BFKL pomeron prediction for the process $\gamma^* + \gamma^* \rightarrow \gamma^* + \gamma^*$ at high energies.

In our calculation all contributions from loop diagrams, i.e., self-energy, triangle, box, and pentagon diagrams, are regulated in dimensional regularization scheme and the ultraviolet divergences are renormalized by adding the corresponding counterterms. In the end, the infrared divergences still exist in the result, which would be canceled after taking account of the real corrections.

We find that for the $\gamma^* + q \rightarrow Q\bar{Q} + q$ process in the massive quark case, the quark mass effects are significant at the next-to-leading order of accuracy, which indicates that for heavy quark diffractive photoproduction, the quark mass is indispensable. Our result might essentially show the quark mass effect, in spite of the absence of real corrections, which are needed in a complete NLO calculation. Moreover, for the photon impact factor with heavy quarks, the photon is legitimate to be real in order to guarantee the perturbative QCD calculations applicable.

ACKNOWLEDGMENTS

This work was supported by the National Natural Science Foundation of China (NSFC) under Grants No. 11905006, No. 11805042, No. 11975236, No. 11635009, and No. 11875071.

APPENDIX A: DEFINITION OF THE LOOP INTEGRALS

The loop integrals in LOOPTOOLS are defined as

$$\begin{aligned}
C_0(p_1^2, p_2^2, p_3^2, (p_1 + p_2)^2, m_1^2, m_2^2, m_3^2) &= \frac{(2\pi\mu)^{4-2\epsilon}}{i\pi^2} \int \frac{d^{4-2\epsilon}q}{[q^2 - m_1^2][(q + p_1)^2 - m_2^2][(q + p_1 + p_2)^2 - m_3^2]}, \\
D_0(p_1^2, p_2^2, (p_1 + p_2)^2, (p_2 + p_3)^2, m_1^2, m_2^2, m_3^2, m_4^2) \\
&= \frac{(2\pi\mu)^{4-2\epsilon}}{i\pi^2} \int \frac{d^{4-2\epsilon}q}{[q^2 - m_1^2][(q + p_1)^2 - m_2^2][(q + p_1 + p_2)^2 - m_3^2][(q + p_1 + p_2 + p_3)^2 - m_4^2]}, \\
\frac{(2\pi\mu)^{4-2\epsilon}}{i\pi^2} \int d^{4-2\epsilon}q \frac{q^\mu}{[q^2 - m_1^2][(q + p_1)^2 - m_2^2][(q + p_1 + p_2)^2 - m_3^2]} &= \sum_{i=1}^2 C_i p_i^\mu, \\
\frac{(2\pi\mu)^{4-2\epsilon}}{i\pi^2} \int d^{4-2\epsilon}q \frac{q^\mu q^\nu}{[q^2 - m_1^2][(q + p_1)^2 - m_2^2][(q + p_1 + p_2)^2 - m_3^2]} &= g^{\mu\nu} C_{00} + \sum_{i,j=1}^2 C_{ij} p_i^\mu p_j^\nu, \\
\frac{(2\pi\mu)^{4-2\epsilon}}{i\pi^2} \int d^{4-2\epsilon}q \frac{q^\mu}{[q^2 - m_1^2][(q + p_1)^2 - m_2^2][(q + p_1 + p_2)^2 - m_3^2][(q + p_1 + p_2 + p_3)^2 - m_4^2]} &= \sum_{i=1}^3 D_i p_i^\mu, \\
\frac{(2\pi\mu)^{4-2\epsilon}}{i\pi^2} \int d^{4-2\epsilon}q \frac{q^\mu q^\nu}{[q^2 - m_1^2][(q + p_1)^2 - m_2^2][(q + p_1 + p_2)^2 - m_3^2][(q + p_1 + p_2 + p_3)^2 - m_4^2]} \\
&= g^{\mu\nu} D_{00} + \sum_{i,j=1}^3 D_{ij} p_i^\mu p_j^\nu, \\
\frac{(2\pi\mu)^{4-2\epsilon}}{i\pi^2} \int d^{4-2\epsilon}q \frac{q^\mu q^\nu q^\rho}{[q^2 - m_1^2][(q + p_1)^2 - m_2^2][(q + p_1 + p_2)^2 - m_3^2][(q + p_1 + p_2 + p_3)^2 - m_4^2]} \\
&= \sum_{i=1}^3 (g^{\mu\nu} p_i^\rho + g^{\nu\rho} p_i^\mu + g^{\mu\rho} p_i^\nu) D_{00i} + \sum_{i,j,k=1}^3 D_{ijk} p_i^\mu p_j^\nu p_k^\rho. \tag{A1}
\end{aligned}$$

All of the coefficients such as C_{ij} , D_{ijk} can be evaluated numerically by LOOPTOOLS.

APPENDIX B: THE LENGTHY AMPLITUDES

In the following, we list the expressions that are not given in the main body of the paper:

$$\begin{aligned}
A_{14} = \Gamma_{qq}^{(0),a} \frac{2s}{t} \left(\frac{ee_f}{s} \right) \left(\frac{N_c}{2} \right) \frac{1}{(4\pi)^2} \{ &H_T^a [3m^2 D_0(14) + 2(3m^2 - t + t_b) D_1(14) \\
&+ (2m^2 + Q^2 - 2t + 2t_a + 4t_b) D_2(14) - 3Q^2 D_3(14) + 6D_{00}(14) + 5m^2 D_{11}(14) \\
&+ (4m^2 + Q^2 - 5t + t_a + 5t_b) D_{12}(14) + 4(m^2 - Q^2 - t_a) D_{13}(14) \\
&+ (m^2 + Q^2 + 4t_b) D_{22}(14) - 2(2m^2 + Q^2 - 2t_b) D_{23}(14) - 3Q^2 D_{33}(14)] \\
&+ m H_{pe}^a [(3m^2 + Q^2 + 2t_a - 2t_b) D_0(14) + (5m^2 + 2Q^2 - 2t + 3t_a) D_1(14) \\
&+ (3m^2 + 3Q^2 - 2t + 4t_a + t_b) D_2(14) - Q^2 D_3(14) + 6D_{00}(14) \\
&+ (4m^2 + Q^2 + t_a) D_{11}(14) + (4m^2 + 3Q^2 - 5t + 2t_a + 4t_b) D_{12}(14) \\
&+ 2(2m^2 - Q^2 - 2t_a) D_{13}(14) + (2m^2 + 2Q^2 + 3t_b) D_{22}(14) \\
&+ 4(t_b - m^2) D_{23}(14) - 3Q^2 D_{33}(14)] \\
&+ H_p^a [\epsilon \cdot r (4m^2 D_1(14) + 2(Q^2 - 3m^2 + 2t_a) D_2(14) - 4Q^2 D_3(14) + 8D_{00}(14) \\
&+ 4m^2 D_{11}(14) - 2(m^2 - Q^2 - t_a) D_{12}(14) + 4(m^2 - Q^2 - t_a) D_{13}(14)]
\end{aligned}$$

$$\begin{aligned}
& -2(m^2 - Q^2 - 2t + t_b)D_{22}(14) + 4(t_a - m^2)D_{23}(14) - 4Q^2D_{33}(14) \\
& - 20D_{002}(14) - 2(m^2 - t + t_b)D_{122}(14) + 2(Q^2 - m^2 + t_a)D_{123}(14) \\
& - 2t_bD_{222}(14) + 2Q^2D_{233}(14) + 2(m^2 + Q^2 - t_b)D_{223}(14) \\
& + \epsilon \cdot k(-6m^2D_0(14) - 2(5m^2 - 2t + 2t_b)D_1(14) - 2(5m^2 - 2t + 2t_b)D_2(14) \\
& - 2Q^2D_3(14) + 4D_{00}(14) + (4t - 6m^2 - 4t_b)D_{11}(14) + 4(t_a - t_b)D_{13}(14) \\
& - 10(m^2 - t + t_b)D_{12}(14) - 2(2m^2 - 2t + 3t_b)D_{22}(14) + 4(t_a - t_b)D_{23}(14) \\
& - 2Q^2D_{33}(14) - 20D_{001}(14) - 20D_{002}(14) - 2(2m^2 - t + t_b)D_{112}(14) \\
& + 2(Q^2 - m^2 + t_a)D_{113}(14) - 2(m^2 - t + 2t_b)D_{122}(14) + 2Q^2D_{133}(14) \\
& + 2(2Q^2 + t_a - t_b)D_{123}(14) - 2t_bD_{222}(14) + 2(m^2 + Q^2 - t_b)D_{233}(14) \\
& + 2Q^2D_{233}(14))] + sH_e^a[-2\alpha m^2D_0(14) + (m^2 + Q^2 - (7m^2 + Q^2)\alpha)D_1(14) \\
& + ((3 - 5\alpha)m^2 + Q^2 + 2t - 2t_a - 2(Q^2 + t_b)\alpha)D_2(14) - 2(1 + 2\alpha)D_{00}(14) \\
& + (m^2 + Q^2(1 + 2\alpha))D_3(14) - ((1 + 3\alpha)m^2 - (1 - \alpha)(Q^2 + t_a))D_{11}(14) \\
& + ((2 - 3\alpha)Q^2 + t_a - t_b - \alpha(3m^2 + 2t_a + 3t_b) + 2(\alpha + 1)t)D_{12}(14) \\
& + ((Q^2 + t_a)(2\alpha + 3) - (1 + 2\alpha)m^2)D_{13}(14) \\
& + (m^2 + Q^2 - t_b - 2\alpha(m^2 + Q^2 + t_b))D_{22}(14) - 2D_{003}(14) \\
& + ((3 + 2\alpha)m^2 + 3Q^2 - (1 + 2\alpha)t_b)D_{23}(14) + 2(1 + \alpha)Q^2D_{33}(14) \\
& + 2(\alpha - 1)(D_{001}(14) + D_{002}(14)) + (\alpha - 1)(2m^2 - t + t_b)D_{112}(14) \\
& + ((\alpha - 2)m^2 + (1 - \alpha)(Q^2 + t_a))D_{113}(14) + (m^2 - t + 2t_b)(\alpha - 1)D_{122}(14) \\
& + (-m^2 + t + (\alpha - 2)t_b - 2Q^2(\alpha - 1) + (1 - \alpha)t_a)D_{123}(14) \\
& + (t_a - m^2 + (2 - \alpha)Q^2)D_{133}(14) + (\alpha - 1)t_bD_{222}(14) \\
& + (m^2 + Q^2 - 2t_b - \alpha(m^2 + Q^2 - t_b))D_{223}(14) \\
& + (m^2 - t_b - Q^2(\alpha - 2))D_{233}(14) + Q^2D_{333}(14)] \\
& + 2mH_m^a[2s((1 + \alpha)D_2(14) + 2D_{12}(14) + (3 - \alpha)D_{22}(14) + (\alpha + 2)D_{23}(14) \\
& + (1 - \alpha)D_{112}(14) + 3(1 - \alpha)D_{122}(14) + (2 - \alpha)D_{123}(14) + 2(1 - \alpha)D_{222}(14) \\
& + (3 - \alpha)D_{223}(14) + 2D_{233}(14))\epsilon \cdot r + 2s(2\alpha D_0(14) + (1 + 3\alpha)D_1(14) + 4\alpha D_2(14) \\
& + 2D_{11}(14) + 4D_{12}(14) + (2 + \alpha)D_{13}(14) + 2D_{22}(14) + (1 + \alpha)D_{23}(14) + D_{133}(14) \\
& + (1 - \alpha)D_{111}(14) + 4(1 - \alpha)D_{112}(14) + (2 - \alpha)D_{113}(14) + 5(1 - \alpha)D_{122}(14) \\
& + (5 - 2\alpha)D_{123}(14) + 2(1 - \alpha)D_{222}(14) + (3 - \alpha)D_{223}(14) + D_{233}(14))\epsilon \cdot k \\
& + (-m^2 + Q^2 + 2t_a)D_0(14) - (2m^2 + 2Q^2 + 3t_a)D_1(14) - (m^2 + 3Q^2 - 2t \\
& + 4t_a + t_b)D_2(14) - (m^2 + Q^2)D_3(14) - 6D_{00}(14) - (Q^2 + t_a)D_{11}(14) \\
& - (3Q^2 - t + 2t_a)D_{12}(14) - 2Q^2D_{13}(14) + (t_b - 2m^2 - 2Q^2)D_{22}(14) \\
& - 4Q^2D_{23}(14) - Q^2D_{33}(14) + 2D_{001}(14) + 4D_{002}(14) + 2D_{003}(14) + m^2D_{111}(14) \\
& + (3m^2 - t + t_b)D_{112}(14) + (2m^2 - Q^2 - t_a)D_{113}(14) + (2m^2 - 2t + 3t_b)D_{122}(14) \\
& + (2m^2 - 3Q^2 - t - 2t_a + 2t_b)D_{123}(14) + (m^2 - 2Q^2 - t_a)D_{133}(14) + 2t_bD_{222}(14) \\
& + (3t_b - 2m^2 - 2Q^2)D_{223}(14) + (t_b - m^2 - 3Q^2)D_{233}(14) - Q^2D_{333}(14))\epsilon \cdot p] \\
& + 2H_k^a[2s((1 - \alpha)D_2(14) + (1 - \alpha)D_{12}(14) - \alpha D_{23}(14) + (\alpha - 1)D_{122}(14) \\
& + (\alpha - 1)D_{123}(14) + (\alpha - 1)D_{222}(14) + (\alpha - 2)D_{223}(14) - D_{233}(14))\epsilon \cdot r
\end{aligned}$$

$$\begin{aligned}
& + 2s((1 - \alpha)D_2(14) - (1 + \alpha)D_{13}(14) - \alpha D_{23}(14) + (\alpha - 1)D_{112}(14) \\
& + (\alpha - 1)D_{113}(14) + 2(\alpha - 1)D_{122}(14) + (2\alpha - 3)D_{123}(14) - D_{133}(14) \\
& + (\alpha - 1)D_{222}(14) + (\alpha - 2)D_{223}(14) - D_{233}(14))\epsilon \cdot k + (2m^2 D_0(14) \\
& + 4m^2 D_1(14) + (m^2 + Q^2 + 2(t_a + t_b - t))D_2(14) + (m^2 - Q^2)D_3(14) \\
& + 2D_{00}(14) + (m^2 + Q^2 - 2t + t_a + 2t_b)D_{12}(14) + (m^2 - Q^2 - t_a)D_{13}(14) \\
& + (m^2 + Q^2 + t_b)D_{22}(14) + (Q^2 - m^2 + t_b)D_{23}(14) - 2D_{002}(14) - 2D_{003}(14) \\
& - m^2 D_{112}(14) - m^2 D_{113}(14) + (t - m^2 - t_b)D_{122}(14) + (Q^2 - 2m^2 + t + t_a \\
& - t_b)D_{123}(14) + (Q^2 - m^2 + t_a)D_{133}(14) - t_b D_{222}(14) + (m^2 + Q^2 - 2t_b)D_{223}(14) \\
& + 2m^2 D_{11}(14) + (m^2 + 2Q^2 - t_b)D_{233}(14) + Q^2 D_{333}(14))\epsilon \cdot p] \\
& - 4mH_{pk}^a[(2(D_0(14) + D_{11}(14) + D_{22}(14)) + 4(D_1(14) + D_2(14) + D_{12}(14)))\epsilon \cdot k \\
& + (D_0(14) + D_1(14) + 3D_2(14) + 2D_{12}(14) + 2D_{22}(14))\epsilon \cdot r] \\
& + 2msH_{ke}^a((1 - 2\alpha)D_0(14) + (2 - 3\alpha)D_1(14) + (2 - 3\alpha)D_2(14) + (1 - \alpha)D_{11}(14) \\
& + 2(1 - \alpha)D_{12}(14) + (1 - \alpha)D_{22}(14) + D_{13}(14) + D_{23}(14)\}.
\end{aligned} \tag{A2}$$

and $D_i(14) = D_i(m^2, t, m^2, -Q^2, t_b, t_a, m^2, 0, 0, m^2)$.

$$\begin{aligned}
A_{12}^0 = & -H_T^a[(3m^2 D_0(12)_{\text{fin}} + (4m^2 - M^2)D_1(12)_{\text{fin}} + m^2 D_{11}(12)_{\text{fin}}) \\
& + (2m^2 + M^2)(D_2(12) + D_{12}(12) + D_{22}(12) - D_{123}(12) - D_{223}(12)) \\
& - 2D_{00}(12) + Q^2 D_{33}(12) - 6D_{003}(12) + Q^2 D_{333}(12) \\
& - (m^2 - Q^2 - t_a)D_{133}(12) - (2m^2 - 2Q^2 - t_a - t_b)D_{233}(12)] \\
& + mH_{pe}^a[-(3m^2 + t_a - t_b)D_0(12)_{\text{fin}} - (4m^2 + 2Q^2 - t + 3t_a)D_1(12)_{\text{fin}} \\
& - (Q^2 + t_a)D_{11}(12)_{\text{fin}} + m^2 D_{111}(12)_{\text{fin}} - (2m^2 + M^2)(D_2(12) + D_{22}(12) \\
& - D_{112}(12) - D_{122}(12) - D_{223}(12)) - (Q^2 + t)D_{12}(12) - 2Q^2 D_{13}(12) \\
& - Q^2 D_{33}(12) + 6D_{001}(12) + 6D_{003}(12) + (2m^2 - Q^2 - t_a)D_{113}(12) \\
& + (4m^2 - 3Q^2 + t - 2t_a - 2t_b)D_{123}(12) + (m^2 - 2Q^2 - t_a)D_{133}(12) \\
& + (2m^2 - 2Q^2 - t_a - t_b)D_{233}(12) - Q^2 D_{333}(12) + 2D_{00}(12)] \\
& + sH_e^a[am^2(D_0(12)_{\text{fin}} + 3D_1(12)_{\text{fin}} + 2D_{11}(12)_{\text{fin}}) + 2\alpha D_{00}(12) \\
& + ((1 + \alpha)m^2 + t - t_a - \alpha(2Q^2 + t_a + t_b))D_2(12) - \alpha Q^2 D_3(12) \\
& + (4am^2 + (1 + \alpha)t - (1 + 2\alpha)t_a - 2\alpha t_b - 3\alpha Q^2)D_{12}(12) \\
& - (2\alpha Q^2 - am^2 + (1 + \alpha)t_a)D_{13}(12) + \alpha(2m^2 - 2Q^2 - t_a - t_b)D_{223}(12) \\
& + ((1 + 4\alpha)m^2 + (1 + \alpha)t - 3\alpha Q^2 - (1 + 2\alpha)t_a - 2\alpha t_b)D_{22}(12) \\
& + ((1 + 2\alpha)m^2 - (1 + \alpha)t_a - \alpha t_b - 4\alpha Q^2)D_{23}(12) - \alpha Q^2 D_{233}(12) \\
& - \alpha Q^2 D_{33}(12) + 2(\alpha - 1)D_{001}(12) - 2(1 - 3\alpha)D_{002}(12) - 2D_{003}(12) \\
& + \alpha(2m^2 + M^2)(D_{122}(12) + D_{222}(12)) + \alpha(m^2 - Q^2 - t_a)D_{123}(12)] \\
& + sH_{ke}^a[(2\alpha - 1)D_0(12)_{\text{fin}} + (3\alpha - 2)D_1(12)_{\text{fin}} \\
& + (\alpha - 1)D_{11}(12)_{\text{fin}} - D_{12}(12) - D_{13}(12)] \\
& + 2mH_{pk}^a[(2D_0(12)_{\text{fin}} + 3D_1(12)_{\text{fin}} + D_{11}(12)_{\text{fin}})\epsilon \cdot k \\
& + (D_0(12)_{\text{fin}} + D_1(12)_{\text{fin}} - D_{12}(12))\epsilon \cdot r] \\
& + 2sH_k^a[(D_2(12) + D_{12}(12) + (1 + \alpha)D_{13}(12) + D_{22}(12) + D_{23}(12)
\end{aligned}$$

$$\begin{aligned}
& + (1 - \alpha)D_{113}(12) + D_{123}(12) + D_{133}(12))\epsilon \cdot k + ((1 - \alpha)(D_2(12) \\
& + D_{12}(12) + D_{22}(12) - D_{123}(12)) - \alpha D_{23}(12) - D_{223}(12) - D_{233}(12))\epsilon \cdot r] \\
& + 2msH_m^a[(-2\alpha D_0(12)_{\text{fin}} - (1 + 3\alpha)D_1(12)_{\text{fin}} - 2D_{11}(12)_{\text{fin}} + (\alpha - 1)D_{111}(12)_{\text{fin}} \\
& - D_2(12) - 2D_{12}(12) - (\alpha + 2)D_{13}(12) - D_{22}(12) - D_{23}(12) - D_{112}(12) \\
& + (\alpha - 2)D_{113}(12) - D_{123}(12))\epsilon \cdot k + ((1 + \alpha)D_2(12) + 2D_{12}(12) + (1 + \alpha)D_{22}(12) \\
& + (2 + \alpha)D_{23}(12) + (1 - \alpha)D_{112}(12) + (2 - \alpha)D_{123}(12) + D_{122}(12) + D_{223}(12) \\
& + D_{233}(12))\epsilon \cdot r] \\
& - 2H_p^a[(-2m^2 D_0(12)_{\text{fin}} - (2m^2 - M^2)D_1(12)_{\text{fin}} + (m^2 + M^2)D_{11}(12)_{\text{fin}} \\
& - (m^2 + Q^2 + t)D_2(12) - (m^2 + Q^2)D_3(12) + (4m^2 - 3Q^2 + t - 2t_a - 2t_b)D_{12}(12) \\
& + 4D_{00}(12) + (2m^2 - 3Q^2 - t_a - t_b)D_{13}(12) + (2m^2 - 2Q^2 - t_a - t_b)D_{22}(22) \\
& + (2m^2 - 4Q^2 - t_a - t_b)D_{23}(12) - 2Q^2 D_{33}(12) + 6D_{002}(12) + 6D_{003}(12) \\
& + (3m^2 + M^2)D_{112}(12) + (2m^2 - Q^2 - t_a)D_{113}(12) + 2(2m^2 + M^2)D_{122}(12) \\
& + (5m^2 - 4Q^2 + t - 3t_a - 2t_b)D_{123}(12) + m^2 D_{111}(12)_{\text{fin}} + (2m^2 + M^2)D_{222}(12) \\
& + (m^2 - 2Q^2 - t_a)D_{133}(12) + (4m^2 - 3Q^2 + t - 2t_a - 2t_b)D_{223}(12) + 4D_{001}(12) \\
& + (2m^2 - 3Q^2 - t_a - t_b)D_{233}(12) - Q^2 D_{333}(12))\epsilon \cdot k + (m^2 D_1(12)_{\text{fin}} + m^2 D_{11}(12)_{\text{fin}} \\
& + (Q^2 - m^2 + t_a)D_2(12) - Q^2 D_3(12) + 2D_{00}(12) - Q^2 D_{33}(12) + 2D_{002}(12) \\
& + (m^2 - Q^2 - t_a)(D_{13}(12) + D_{22}(12)) + (m^2 - 2Q^2 - t_a)D_{23}(12))\epsilon \cdot r] \\
& + 2\epsilon \cdot p H_k^a[-m^2 D_0(12)_{\text{fin}} - 2m^2 D_1(12)_{\text{fin}} - m^2 D_{11}(12)_{\text{fin}} - (2m^2 + M^2) \\
& \times (D_2(12) + D_{12}(12) + D_{22}(12) - D_{123}(12) - D_{223}(12)) - m^2 D_3(12) - Q^2 D_{33}(12) \\
& + 4D_{003}(12) + m^2 D_{113}(12) + (2m^2 - 2Q^2 - t_a - t_b)D_{233}(12) - Q^2 D_{333}(12) \\
& + (m^2 - Q^2 - t_a)D_{133}(12)] \\
& + 2mH_m^a\epsilon \cdot p[(m^2 + Q^2 + t_a)D_0(12)_{\text{fin}} + (m^2 + 2Q^2 + 2t_a)D_1(12)_{\text{fin}} \\
& + (Q^2 - m^2 + t_a)D_{11}(12)_{\text{fin}} - m^2 D_{111}(12)_{\text{fin}} + (Q^2 + t)D_2(12) \\
& + (m^2 + 2Q^2)D_3(12) + (2Q^2 - 2m^2 + t_a + t_b)D_{12}(12) + 2Q^2 D_{33}(12) \\
& - (m^2 - 3Q^2 - t_a)D_{13}(12) - (2m^2 - 2Q^2 - t_a - t_b)D_{23}(12) - 4D_{001}(12) \\
& - (2m^2 + M^2)(D_{112}(12) + D_{122}(12) + D_{223}(12)) + (Q^2 - 2m^2 + t_a)D_{113}(12) \\
& - (4m^2 - 3Q^2 + t - 2t_a - 2t_b)D_{123}(12) - (m^2 - 2Q^2 - t_a)D_{133}(12) \\
& - 4D_{003}(12) + (2Q^2 - 2m^2 + t_a + t_b)D_{233}(12) + Q^2 D_{333}(12)]. \tag{A3}
\end{aligned}$$

Here $D_i(12) = D_i(m^2, m^2, t, -Q^2, 2m^2 + M^2, t_a, m^2, 0, m^2, m^2)$.

$$\begin{aligned}
\bar{A}_{12}^0 &= -H_T^a[(3m^2 D_0(\overline{12})_{\text{fin}} + (4m^2 - M^2)D_1(\overline{12})_{\text{fin}} + m^2 D_{11}(\overline{12})_{\text{fin}}) \\
&+ (2m^2 + M^2)(D_2(\overline{12}) + D_{12}(\overline{12}) + D_{22}(\overline{12}) - D_{123}(\overline{12}) - D_{223}(\overline{12})) \\
&- 2D_{00}(\overline{12}) + Q^2 D_{33}(\overline{12}) - 6D_{003}(\overline{12}) - (m^2 - Q^2 - t_b)D_{133}(\overline{12}) \\
&- (2m^2 - 2Q^2 - t_b - t_a)D_{233}(\overline{12}) + Q^2 D_{333}(\overline{12})] \\
&- mH_{pe}^a[(3m^2 + t_a - t_b)D_0(\overline{12})_{\text{fin}} + (4m^2 - t + 2t_a - t_b)D_1(\overline{12})_{\text{fin}} \\
&+ (2m^2 - Q^2 - t_b)D_{11}(\overline{12})_{\text{fin}} + m^2 D_{111}(\overline{12})_{\text{fin}} + m^2 D_3(\overline{12}) \\
&+ (2m^2 + M^2)(D_2(12) + D_{22}(12) + D_{112}(\overline{12}) + D_{122}(\overline{12}) - D_{223}(\overline{12}))
\end{aligned}$$

$$\begin{aligned}
& + (4m^2 - 3Q^2 + t - 2t_a - 2t_b)D_{12}(\overline{12}) - 2Q^2D_{13}(\overline{12}) + Q^2D_{33}(\overline{12}) \\
& + 6D_{001}(\overline{12}) - 6D_{003}(\overline{12}) - (Q^2 + t_b)D_{113}(\overline{12}) - (Q^2 + t)D_{123}(\overline{12}) \\
& + (m^2 - t_b)D_{133}(\overline{12}) - (2m^2 - 2Q^2 - t_a - t_b)D_{233}(\overline{12}) + Q^2D_{333}(\overline{12})] \\
& + sH_e^a[(\alpha + 2)m^2D_0(\overline{12})_{\text{fin}} + ((3\alpha + 1)m^2 - M^2)D_1(\overline{12})_{\text{fin}} \\
& + (2\alpha - 1)m^2D_{11}(\overline{12})_{\text{fin}} + (\alpha m^2 + (1 - 2\alpha)Q^2 - \alpha t_a + (1 - \alpha)t_b)D_2(\overline{12}) \\
& + (m^2 + (1 - \alpha)Q^2)D_3(\overline{12}) + 2(\alpha - 2)D_{00}(\overline{12}) \\
& + (2(2\alpha - 1)m^2 + (2 - 3\alpha)Q^2 + (\alpha - 1)(t + 2t_b) + (1 - 2\alpha)t_a)D_{12}(\overline{12}) \\
& + (2(1 - \alpha)Q^2 + (\alpha - 1)m^2 + (2 - \alpha)t_b)D_{13}(\overline{12}) \\
& + ((4\alpha - 3)m^2 + (\alpha - 1)t + (2 - 3\alpha)Q^2 + (1 - 2\alpha)t_a + 2(1 - \alpha)t_b)D_{22}(\overline{12}) \\
& + ((2\alpha - 3)m^2 + (1 - \alpha)t_a + (2 - \alpha)t_b - 4(1 - \alpha)Q^2)D_{23}(\overline{12}) \\
& + (2 - \alpha)Q^2D_{33}(\overline{12}) + 2\alpha D_{001}(\overline{12}) + 2(3\alpha - 2)D_{002}(\overline{12}) - 4D_{003}(\overline{12}) \\
& + (\alpha - 1)(2m^2 + M^2)(D_{122}(\overline{12}) + D_{222}(\overline{12})) + (Q^2 - m^2 + t_b)D_{133}(\overline{12}) \\
& + (2(\alpha - 2)m^2 + (3 - 2\alpha)Q^2 - t + (2 - \alpha)(t_a + t_b))D_{223}(\overline{12}) \\
& + ((\alpha - 3)m^2 + (2 - \alpha)Q^2 - t + t_a + (2 - \alpha)t_b)D_{123}(\overline{12}) + (\alpha - 1)m^2D_{112}(\overline{12}) \\
& + ((3 - \alpha)Q^2 - 2m^2 + t_a + t_b)D_{233}(\overline{12}) + Q^2D_{333}(\overline{12}) - m^2D_{113}(\overline{12})] \\
& + sH_{ke}^a[(2\alpha - 1)D_0(\overline{12})_{\text{fin}} + (3\alpha - 1)D_1(\overline{12})_{\text{fin}} + \alpha D_{11}(\overline{12})_{\text{fin}} + D_{12}(\overline{12}) \\
& + D_{13}(\overline{12})] + 2mH_{pk}^a[(2D_0(\overline{12})_{\text{fin}} + 3D_1(\overline{12})_{\text{fin}} + D_{11}(\overline{12})_{\text{fin}})\epsilon \cdot k \\
& + (D_0(\overline{12})_{\text{fin}} + 2D_1(\overline{12})_{\text{fin}} + D_{11}(\overline{12})_{\text{fin}} + D_{12}(\overline{12}))\epsilon \cdot r] \\
& + 2sH_k^a[(D_2(\overline{12}) + D_{12}(\overline{12}) + (2 - \alpha)D_{13}(\overline{12}) + D_{22}(\overline{12}) \\
& + D_{23}(\overline{12}) + \alpha D_{113}(\overline{12}) + D_{123}(\overline{12}) + D_{133}(\overline{12}))\epsilon \cdot k \\
& + ((1 - \alpha)(D_2(\overline{12}) + D_{12}(\overline{12}) + D_{22}(\overline{12})) + \alpha D_{113}(\overline{12}) + D_{133}(\overline{12}) \\
& + (2 - \alpha)(D_{13}(\overline{12}) + D_{23}(\overline{12})) + (1 + \alpha)D_{123}(\overline{12}) + D_{223}(\overline{12}) + D_{233}(\overline{12}))\epsilon \cdot r] \\
& + 2msH_m^a[(-2\alpha D_0(\overline{12})_{\text{fin}} + (1 - 3\alpha)D_1(\overline{12})_{\text{fin}} + D_{11}(\overline{12})_{\text{fin}} + \alpha D_{111}(\overline{12})_{\text{fin}} \\
& - D_2(\overline{12}) - (1 - \alpha)D_{13}(\overline{12}) - D_{22}(\overline{12}) - D_{23}(\overline{12}) + D_{112}(\overline{12}) + (1 - \alpha)D_{113}(\overline{12}) \\
& - D_{123}(\overline{12}) - D_{133}(\overline{12}))\epsilon \cdot k + (D_1(\overline{12})_{\text{fin}} + (1 + \alpha)D_{11}(\overline{12})_{\text{fin}} + \alpha D_{111}(\overline{12})_{\text{fin}} \\
& - D_2(\overline{12}) + (1 + \alpha)(2D_{12}(\overline{12}) + D_{22}(\overline{12}) + D_{112}(\overline{12})) + (1 - \alpha)D_{113}(\overline{12}) \\
& + \alpha D_{23}(\overline{12}) - \alpha D_{123}(\overline{12}) + D_{122}(\overline{12}) - D_{133}(\overline{12}) - D_{223}(\overline{12}) - D_{233}(\overline{12}))\epsilon \cdot r] \\
& - 2H_p^a[(-2m^2D_0(\overline{12})_{\text{fin}} - (2m^2 - M^2)D_1(\overline{12})_{\text{fin}} + (m^2 + M^2)D_{11}(\overline{12})_{\text{fin}} \\
& + m^2D_{111}(\overline{12})_{\text{fin}} - (m^2 + Q^2 + t)D_2(\overline{12}) - (m^2 + Q^2)D_3(\overline{12}) + 4D_{00}(\overline{12}) \\
& + (4m^2 - 3Q^2 + t - 2t_a - 2t_b)D_{12}(\overline{12}) + (2m^2 - 3Q^2 - t_a - t_b)D_{13}(\overline{12}) \\
& + 4D_{001}(\overline{12}) + (2m^2 - 2Q^2 - t_a - t_b)D_{22}(\overline{12}) + 6D_{002}(\overline{12}) + 6D_{003}(\overline{12}) \\
& + (2m^2 - 4Q^2 - t_a - t_b)D_{23}(\overline{12}) - 2Q^2D_{33}(\overline{12}) + (3m^2 + M^2)D_{112}(\overline{12}) \\
& + (2m^2 - Q^2 - t_b)D_{113}(\overline{12}) + (5m^2 - 4Q^2 + t - 2t_a - 3t_b)D_{123}(\overline{12}) \\
& + (m^2 - 2Q^2 - t_b)D_{133}(\overline{12}) + (4m^2 - 3Q^2 + t - 2t_a - 2t_b)D_{223}(\overline{12}) \\
& + 2(2m^2 + M^2)D_{122}(\overline{12}) + (2m^2 + M^2)D_{222}(\overline{12}) - Q^2D_{333}(\overline{12}) \\
& + (2m^2 - 3Q^2 - t_a - t_b)D_{233}(\overline{12}))\epsilon \cdot k \\
& + (m^2D_0(\overline{12})_{\text{fin}} + m^2D_1(\overline{12})_{\text{fin}} + m^2D_{11}(\overline{12})_{\text{fin}} + m^2D_{111}(\overline{12})_{\text{fin}})
\end{aligned}$$

$$\begin{aligned}
& - (Q^2 + t_a)D_2(\overline{12}) + (4m^2 - 3Q^2 + 2t - 3t_a - 2t_b)D_{12}(\overline{12}) \\
& + (m^2 - 2Q^2 - t_a)D_{13}(\overline{12}) + (3m^2 - 2Q^2 + t - 2t_a - t_b)D_{22}(\overline{12}) \\
& + (m^2 - 2Q^2 - t_a)D_{23}(\overline{12}) + 4D_{001}(\overline{12}) + (3m^2 + M^2)D_{112}(\overline{12}) \\
& + 4D_{002}(\overline{12}) + (m^2 - Q^2 - t_b)D_{113}(\overline{12}) + 2(2m^2 + M^2)D_{122}(\overline{12}) \\
& + (3m^2 - 3Q^2 - t_a - 2t_b)D_{123}(\overline{12}) + (2m^2 + M^2)D_{222}(\overline{12}) \\
& + (2m^2 - 2Q^2 - t_a - t_b)D_{223}(\overline{12}) - Q^2D_{133}(\overline{12}) - Q^2D_{233}(\overline{12})\epsilon \cdot r] \\
& + 2\epsilon \cdot p H_k^a [-2m^2D_0(\overline{12})_{\text{fin}} - (2m^2 - M^2)D_1(\overline{12})_{\text{fin}} + 2D_{00}(\overline{12})_{\text{fin}} + 2D_{003}(\overline{12})_{\text{fin}}] \\
& + 2mH_m^a \epsilon \cdot p [(2m^2 + Q^2 + t_a)D_0(\overline{12})_{\text{fin}} + (m^2 + 2Q^2 - t + 2t_a + t_b)D_1(\overline{12})_{\text{fin}} \\
& - m^2D_{11}(\overline{12})_{\text{fin}} - (2m^2 - 2Q^2 - t_a - t_b)D_2(\overline{12}) + 2Q^2D_3(\overline{12}) - 2D_{00}(\overline{12}) \\
& + (Q^2 - 2m^2 - t + t_a + t_b)D_{12}(\overline{12}) - (2m^2 - 2Q^2 - t_a - t_b)D_{23}(\overline{12}) \\
& + (Q^2 - m^2 + t_b)D_{13}(\overline{12}) + Q^2D_{33}(\overline{12}) + 2D_{001}(\overline{12}) - 2D_{003}(\overline{12})]. \tag{A4}
\end{aligned}$$

Here $D_i(\overline{12}) = D_i(m^2, m^2, -Q^2, t, 2m^2 + M^2, t_b, m^2, 0, m^2, m^2)$.

$$\begin{aligned}
A_{13}^{(0)} = & H_T^a \{ \alpha(\alpha-1)t(t_a - t_b)[(\alpha-1)sD_0(2) - \alpha sD_0(1)] \\
& - (\alpha-1)(2\Delta + (\alpha-1)\alpha(t_a - t_b)(t_a - m^2))sD_0(3) \\
& - \alpha(2\Delta + (\alpha-1)\alpha(t_b - t_a)(t_b - m^2))sD_0(4) \\
& - [2(\alpha-1)\alpha m^6 + m^4(2(\alpha^2 - \alpha - 1)t - 3(\alpha-1)\alpha(t_a + t_b))] \\
& + m^2(2t(\alpha(\alpha-1)Q^2 - \alpha(\alpha-2)t_a + (1-\alpha^2)t_b) - 2t^2 \\
& + (\alpha-1)\alpha(t_a^2 + 4t_a t_b + t_b^2)) + (\alpha-1)\alpha(2t - t_a - t_b)(Q^2t + t_a t_b)]D_0(14)\} \\
& + (sH_\epsilon^a - 2(H_k^a - mH_m)\epsilon \cdot p)\{t(\alpha-1)\alpha(t_a - m^2)(\alpha sD_0(1) - (\alpha-1)sD_0(2)) \\
& - \alpha(-\Delta + m^2t - (\alpha-1)\alpha Q^2 t)sD_0(4) + (\alpha-1)^2\alpha(t_a - m^2)^2sD_0(3) \\
& - [-(\alpha-1)\alpha m^6 + \alpha m^4((\alpha-1)(2t_a + t_b) - 2(\alpha-2)t)] \\
& + m^2(\alpha t(-(\alpha-1)Q^2 + 2\alpha(t_a + t_b) - 2(2t_a + t_b)) + 2t^2 - (\alpha-1)\alpha t_a(t_a + 2t_b)) \\
& - (\alpha-1)\alpha(2t - t_a)(Q^2t + t_a t_b)]D_0(14)\} \\
& + 2t\Delta(H_T^a + mH_{pe}^a - sH_\epsilon^a - 2H_p^a\epsilon \cdot k + 2(H_k^a - mH_m^a)\epsilon \cdot p)D_0(14) \\
& + mH_{pe}^a \{t(t - (\alpha-1)\alpha(t_a - t_b))(\alpha sD_0(1) - (\alpha-1)sD_0(2)) \\
& - [2(\alpha-1)\alpha m^4 - m^2(3t + (\alpha-1)\alpha(t_a + 3t_b))] \\
& + t(2(\alpha-1)\alpha Q^2 + t_b) + (\alpha-1)\alpha t_b(t_a + t_b)]\alpha sD_0(4) \\
& - [2(\alpha-1)\alpha m^4 - m^2(t + (\alpha-1)\alpha(t_b + 3t_a))] \\
& + t(2(\alpha-1)\alpha Q^2 - t_a) + (\alpha-1)\alpha t_a(t_a + t_b)](\alpha-1)sD_0(3) \\
& - [2(\alpha-1)\alpha m^6 + m^4(t(2\alpha^2 - 4\alpha - 1) - 3(\alpha-1)\alpha(t_a + t_b))] \\
& + m^2(t(-2\alpha^2(t_a + t_b - Q^2) + 2\alpha(3t_a + t_b - Q^2) - t_a + t_b) \\
& - 2t^2 + (\alpha-1)\alpha(t_a^2 + 4t_a t_b + t_b^2)) \\
& + (Q^2t + t_a t_b)((2\alpha^2 - 4\alpha + 1)t - (\alpha-1)\alpha(t_a + t_b))]D_0(14)\} \\
& + 2mtH_{pk}^a \epsilon \cdot p \{-\alpha tD_0(1) + (\alpha-1)tD_0(2) \\
& + \alpha(t_b - m^2)D_0(4) - (\alpha-1)(t_a - m^2)D_0(3) \\
& + (1-2\alpha)(m^4 - m^2(t_a + t_b) + Q^2t + t_a t_b)D_0(14)/s\}
\end{aligned}$$

$$\begin{aligned}
& + 2H_p^a \{ t(\alpha(\alpha-1)s(m^2-t_a)\epsilon \cdot r - tm^2\epsilon \cdot p) \alpha D_0(1) \\
& + t(\alpha(\alpha-1)s(t_a-m^2)\epsilon \cdot r + tm^2\epsilon \cdot p)(\alpha-1)D_0(2) \\
& + (t_a-m^2)(\alpha(\alpha-1)s(m^2-t_a)\epsilon \cdot r - tm^2\epsilon \cdot p)(\alpha-1)D_0(3) \\
& - (s(\Delta-m^2t+(\alpha-1)\alpha Q^2t)\epsilon \cdot r + m^2t(m^2-t_b)\epsilon \cdot p)\alpha D_0(4) \\
& - [(2\alpha-1)m^2t(m^4-m^2(t_a+t_b)+Q^2t+t_at_b)\epsilon \cdot p/s \\
& + (m^2-t_a)(\Delta+m^2t(1-2\alpha))\epsilon \cdot r - 2t\Delta\epsilon \cdot k]D_0(14) \\
& - 2t\Delta\epsilon \cdot k(D_1(14) + D_2(14)) - 2t\Delta\epsilon \cdot rD_2(14) \}.
\end{aligned} \tag{A5}$$

and

$$\begin{aligned}
D_0(1) &= D_0(m^2, 0, 0, t_a, \alpha s, t, m^2, 0, 0, 0)_{\text{fin}} \\
D_0(2) &= D_0(m^2, 0, 0, t_b, (\alpha-1)s, t, m^2, 0, 0, 0)_{\text{fin}} \\
D_0(3) &= D_0(m^2, 0, \alpha s, -Q^2, (\alpha-1)s, t_a, m^2, 0, 0, m^2)_{\text{fin}} \\
D_0(4) &= D_0(m^2, 0, (\alpha-1)s, -Q^2, \alpha s, t_b, m^2, 0, 0, m^2)_{\text{fin}}.
\end{aligned} \tag{A6}$$

$D_i(14)$ is defined in the above paragraphs. The finite parts of these four-point integrals can also be obtained from [28], or evaluated by LOOPTOOLS numerically.

- [1] E. Levin, arXiv:hep-ph/9808486.
- [2] P. V. Landshoff, arXiv:hep-ph/0108156.
- [3] V. A. Petrov and A. V. Prokudin, Eur. Phys. J. C **23**, 135 (2002).
- [4] V. S. Fadin, R. Fiore, and A. Quartarolo, Phys. Rev. D **50**, 2265 (1994).
- [5] V. S. Fadin, D. Ivanov, and M. Kotsky, arXiv:hep-ph/0007119.
- [6] F. Yuan and K. T. Chao, Phys. Rev. D **60**, 094012 (1999).
- [7] F. Yuan and K. T. Chao, Phys. Rev. D **58**, 114016 (1998).
- [8] V. S. Fadin and L. N. Lipatov, Phys. Lett. B **429**, 127 (1998).
- [9] J. Bartels, A. De Roeck, and H. Lotter, Phys. Lett. B **389**, 742 (1996).
- [10] S. J. Brodsky, F. Hautmann, and D. E. Soper, Phys. Rev. D **56**, 6957 (1997); Phys. Rev. Lett. **78**, 803 (1997).
- [11] M. Koratzinos, arXiv:1501.06854.
- [12] ILC, Basic Conceptual Design Report, <http://www.linearcollider.org>.
- [13] A. Accardi *et al.*, Eur. Phys. J. A **52**, 268 (2016).
- [14] D. P. Anderle *et al.*, Front. Phys. (Beijing) **16**, 64701 (2021).
- [15] J. Bartels, C. Ewerz, and R. Staritzbichler, Phys. Lett. B **492**, 56 (2000).
- [16] A. Donnachie and S. Söldner-Rembold, J. Phys. G **26**, 689 (2000).
- [17] S. J. Brodsky, V. S. Fadin, V. T. Kim, L. N. Lipatov, and G. B. Pivovarov, JETP Lett. **70**, 155 (1999).
- [18] M. Ciafaloni and G. Camici, Phys. Lett. B **430**, 349 (1998).
- [19] S. Gieseke, Nucl. Phys. **B121**, 42 (2003).
- [20] J. Bartels, D. Colferai, S. Gieseke, and A. Kyrieleis, Phys. Rev. D **66**, 094017 (2002).
- [21] J. Bartels, Nucl. Phys. **B116**, 126 (2003).
- [22] J. Bartels, S. Gieseke, and C. F. Qiao, Phys. Rev. D **63**, 056014 (2001); **65**, 079902(E) (2002).
- [23] T. Hahn, Comput. Phys. Commun. **140**, 418 (2001).
- [24] R. Metig, M. Böhm, and A. Denner, Comput. Phys. Commun. **64**, 345 (1991).
- [25] T. Hahn and M. Pérez-Victoria, Comput. Phys. Commun. **118**, 153 (1999).
- [26] A. Denner and S. Dittmaier, Nucl. Phys. **B658**, 175 (2003).
- [27] See Supplemental Material at <http://link.aps.org/supplemental/10.1103/PhysRevD.106.034027> for Mathematica code, readers can copy them to the Mathematica page to use directly. When using the results, the high energy package FEYNCALC and the loop integral package LOOPTOOLS are needed.
- [28] R. Keith Ellis and Giulia Zanderighi, J. High Energy Phys. 02 (2008) 002.